

# Modeling Plant Structures Using Concept Sketches

Fabricio Anastacio<sup>1</sup>

Mario Costa Sousa<sup>1</sup>

Faramarz Samavati<sup>1</sup>

Joaquim A. Jorge<sup>2</sup>

<sup>1</sup>University of Calgary

<sup>2</sup>Technical University of Lisbon

## Abstract

Creating 3D plant models is often a hard and laborious task. To make it easier and more natural, we propose a sketch-based interface for modeling single-compound plant structures with phyllotactic arrangements. Our approach is based on the traditional illustration technique of concept sketching. The user sketches the key construction lines for the main plant body and lateral organs. Our system then automatically constructs the 3D plant arrangement in phyllotactic patterns rendered as pen-and-ink line drawings. The user is then able to edit the model by oversketching the construction lines, adjusting density of lateral organs, and specifying different phyllotactic patterns. We demonstrate the capabilities of our system for a variety of plant models.

**CR Categories:** I.3.5 [Computer Graphics]: Computational Geometry and Object Modeling: —Modeling packages; J.5 [Arts and Humanities]: Fine Arts: —Illustration

**Keywords:** sketch-based interface and modeling, concept sketch, plant modeling, phyllotaxis, non-photorealistic rendering

## 1 Introduction

Illustrators are increasingly using 3D modeling tools (i.e., Maya, Poser) as part of the digital illustration production pipeline, primarily to create 3D representations from preliminary drawings [Hodges 2003]. However, most illustrators agree that available methods of constructing, editing and manipulating 3D models (i.e., control points manipulation, multiple menus, parameter adjustment, etc.) do not lend to a natural interaction metaphor and force them to diverge from their preferred ways of thinking and working [Sousa 2005]. Sketch-based interfaces and modeling (SBIM) approaches can potentially offer natural solutions to these problems. The main goal of SBIM systems is to allow the creation, manipulation and subsequent annotation of 3D models by using strokes extracted from user input and/or existing drawing scans [Naya et al. 2002] and interpreted according to artistic principles and techniques of form depiction [Rawson 1987].

Recently, there has been a growing relation being established by researchers between NPR and SBIM whereby SBIM can be thought of as *Inverse NPR* [Nealen et al. 2005], in which feature lines typically extracted from given 3D models (i.e., silhouettes, suggestive contours, ridges) are used to construct new or augment existing 3D models instead. Moreover, illustrators strongly agree that SBIM and NPR approaches should be key components of a digital illustration production pipeline from concept sketches, model construction and expressive rendering [Sousa 2005].

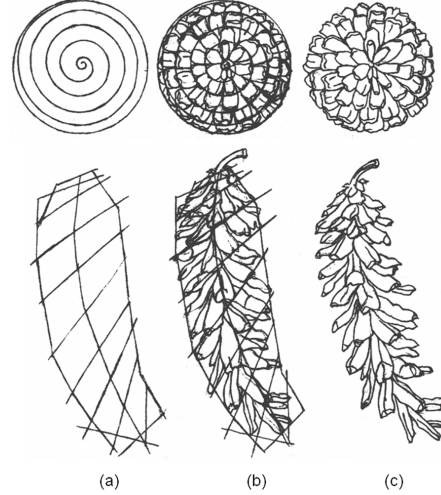


Figure 1: Top and lateral concept drawing progression of a white pine cone. (a) Construction lines are sketched defining the spiral phyllotactic pattern and overall shape of plant; (b) the basic shape of the lateral organs (pine needles) are sketched following the path, inclination and area coverage as indicated by the construction lines; (c) the drawing is now ready for additional refinements after construction lines are erased. Copyright 1991 Eleanor B. Wunderlich. Used by permission.

One area that can benefit from using SBIM approaches is plant modeling for 3D content creation in art, production and science. Plants have a very intricate structure, which makes their 3D modeling a rather laborious task. Although very effective simulation-based modeling approaches exist [Jirasek et al. 2000; Mech and Prusinkiewicz 1996; Prusinkiewicz and Lindenmayer 1990], they require the modeller to have a good understanding of the underlying botanical and biological processes and often result in long modeling and simulation times.

In this paper, we present a novel SBIM method to construct and edit 3D *single-compound* plant structures (sequence of organs supported by a single stem) arranged in different *phyllotactic* patterns such as spiral and other alternate modes. We were inspired by botanical illustration techniques used for preliminary *concept* drawings of such plant arrangements, in particular the lateral layered technique illustrated in Figure 1. Concept drawings convey ideas about how to solve the problem, but they do not involve the level of detail that goes into final drawings. They are used at the very beginning of the illustration process to quickly indicate posture, proportions, topology and constraints [Hodges 2003; Wunderlich 1991].

In our approach (Figure 2), the user sketches (a) the main plant body (Section 3) and (b) a pair of lateral organ structures (i.e., leaves, petals) (Section 4). Our system then automatically computes (c) 3D organs surfaces and their shape variations (Section 4). (d) Organ branching line references are then automatically positioned in the plant using phyllotactic rules (Sections 5, 6), resulting in a 3D representation of the 2D concept drawing given in (a). Finally, the complete plant arrangement is composed by first mapping the plant

organ surfaces of (c) in the branch positions of (d) and then rendering the complete plant model as pen-and-ink lines (e) (Section 7).

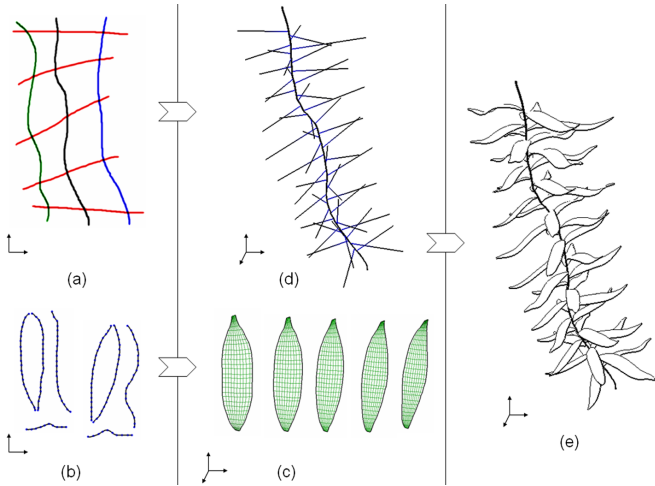


Figure 2: Overview of our approach. User sketches (a) plant main body and (b) lateral organs (i.e. leaves, petals) and the system automatically computes the 3D representations of (c) organ surfaces and their variations, (d) organ branch positioning and (e) final composition by mapping the organ surfaces of (c) in the organ positions of (d), and then rendering the complete plant model in pen-and-ink.

Our main contribution is on providing a concept sketch-based interface and modeling for 3D single-compound plant structures with phyllotactic arrangements and having hand-gestures artistic variations with biologically-correct positioning rules of plant organs.

The rest of this paper is organized as follows: related research is reviewed in Section 2, details of our approach are provided in Sections 3 to 7, results are discussed in Section 8, and conclusions presented in Section 9.

## 2 Related work

**Interactive plant modeling** The main inspiration for our work comes from the approach proposed by Prusinkiewicz *et al.* [2001]. They used artistic principles of plant drawing composition to improve the interface of simulation-based environments, showing that L-system plant modeling can be made more intuitive using functions that control positional information. These user-defined functions are splines that can describe the plant posture and the distribution of components along the plant axes, mapping it to *morphogenetic gradients*. The plant silhouette can also be controlled by bounding the extent of first-order branches for certain types of trees. Although this technique gives an important step towards making L-systems easier to employ, mathematical functions are still hard and too abstract for many of the potential users. In their implementation, the user manipulates function plots that are displayed separately from the model. Our work provides a more direct manipulation interface, in which the user interacts with the modeled structure itself, leading to a more natural modeling process.

Using a broader range of positional information and an intended more intuitive set of parameters, Weber and Penn [1995] introduce a different approach to plant modeling. Their proposal focuses in the overall geometrical structure of the tree, instead of following botanical principles. They additionally describe a technique for adapting

the tree rendering according to the viewer distance, allowing better performance for drawing forests and landscapes with a large number of trees. Even though they avoid using complex mathematical and botanical principles for tree modeling, a large number of parameters needs to be defined by the user.

Lintermann and Deussen [1999] describe another modeling system that combines a rule-based approach with interactive editing of function plots to create the plant models. They also favour overall appearance instead of botanical accuracy. The system, called *Xfrog* ([www.xfrog.com](http://www.xfrog.com)), can even be used for generating non-botanical objects, besides a wide range of plants. Their approach is based in a graph representation of the model. The nodes of the graph are components that describe parts of a plant and the edges correspond to creation dependencies. The program allows a high level of interaction and fast feedback, but still demands the user to deal with function plots and potentially complex data structures.

To facilitate editing plants created with L-systems, Boudon *et al.* [2003] propose multiscale representations of plant structures using *decomposition graphs*. This allows the user to model plants in a global-to-local fashion, manipulating parameters stored in the graph nodes. The plant silhouette can also be defined through an interface based on control points and curvature manipulation for the main axis and the envelope. Bonsai trees are modeled to demonstrate the technique. Even though it makes easier controlling all the parameters involved in L-system plant modeling, a good understanding of the plant structure and of how the parameters behave in the graph topology are needed. The silhouette is the only feature modeled graphically but still using a control point paradigm.

**SBIM of plants** Since 1994, there has been a consistent number of works focusing on NPR of plants [Strothotte *et al.* 1994; Salisbury *et al.* 1997; Deussen and Strothotte 2000; Secord 2002; Di Fiore *et al.* 2003; Sousa and Prusinkiewicz 2003]. SBIM of plants, the main focus of our work, however, has only received attention more recently.

Ijiri *et al.* [2005] present a SBIM system used together with *floral diagrams* and *inflorescences* to provide quick and easy creation of flowers. The floral receptacle and the floral components are modeled by sketching. Several techniques (like surface of revolution, inflation, and sweeping) are specifically used for the 3D interpretation of the sketch of each different component. Their system establishes a clear separation between the general structure definition and the geometrical modeling of individual components. We share this methodology, using an artistic-inspired sketch-based approach for the structure definition as well, combining it with some botanical rules.

Okabe and Igarashi [2003] present a system that creates 3D trees from freehand sketched lines using Weber and Penn [1995] prediction patterns. The generated 3D model can be interactively edited. In a more recent work, Okabe *et al.* [2005] also rely on directly specifying shapes. But, in this one, they try to facilitate modeling by offering example-based editing modes.

**SBIM using construction lines** Pereira *et al* [2004], apply construction lines to help in drafting geometrical drawings, much in the same way that drafts people work. In their system, construction lines do not necessarily become part of the finished drawing. Rather, they help in specifying constraints, geometrical parameters, etc. without the need to specify lower-level details such as dimensions. The authors call it an *incremental drawing paradigm*.

The Teddy system [Igarashi *et al.* 1999] also uses auxiliary lines to specify areas of influence (scope) and geometric deformation operators. In a similar approach Igarashi's *Chateau* system [Igarashi

and Hughes 2001] uses suggestions, a form of dynamic menus, to help users perform constrained drawings using a modicum of input.

Cherlin *et al.* [2005] present a SBIM system for general free form parametric surfaces with examples and operators well suited for plant modeling. They also use auxiliary lines for specifying deformation operations in the 3D models.

Yang *et al.* [2005] introduce a SBIM technique for the creation of 3D objects from pre-defined 2D sketch templates. A graph hierarchical representation for sketches and templates is used. They try then to match the representation of the former to some instance of the representation of the latter. Matching is done using curve feature vectors coupled with a scoring function. If the matching is successful, the selected template determines how to create the 3D model using information (such as dimensions, position of parts, etc.) extracted from the sketch to parameterize the process.

### 3 Plant structure

This is the first stage of interaction with our system (Figure 2(a)). The user draws the 2D construction lines that define the overall posture and structure of the plant arrangement. These lines are then recorded and re-sampled to provide a structured description of the drawing.

In this first stage, the user follows the same steps and procedures performed by an illustrator, as described in Section 1 and Figure 1(a). In our system, the user sketches three groups of construction lines in this order: *stem*, *boundary* and *inclination* lines. The stem line (middle line, in black) defines the main plant stem in which lateral organs are automatically placed later on (Section 6). Boundary lines (left and right lines, in green and blue, respectively) define the lateral extent of the plant organs. Inclination lines (cross-section lines, in red) cross the stem and boundary lines and define the inclination of plant organs along the stem. The region between two consecutive inclination lines is called a *layer*. After sketching, the resulting shapes of all three groups of lines are always planar. Figure 3 shows three examples of these three groups of lines and the effects on the branching inclination and extent along the stem.

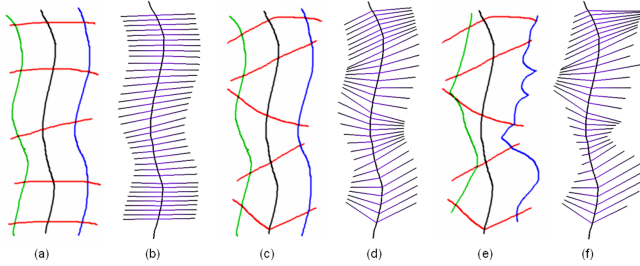


Figure 3: Conceptual drawing of a plant structure defined by three groups of construction lines: stem, boundary and inclination: (a) original drawing, (c) editing the inclination and then (e) the boundary lines. Illustrations in (b, d, f) show the overall 2D effect of the extent and inclination of branches to the left and right of the stem as a result of the configuration of the construction lines in (a, c, e).

Our system captures the input pixels in the screen while the user sketches each line using a mouse or tablet. Each of these points is sequentially added to a collection inside a *Stroke* object assigned to each separate construction line. These input points are usually too sparse (due to hand motions and device artefacts), so the line needs to be re-sampled. The method used consists in adding points by

linear interpolation along the lines between two consecutive input points in order to have a desired density. After this adjustment in the resolution, the stroke is rendered as a line strip passing along the new sequence of points.

### 4 Lateral plant organs

The second interactive session of our system (Figure 2(b)) deals with the creation of lateral plant organs. These can be leaves, petals, or other similar structures. The concept drawing of these organs is defined by four strokes: two for boundaries, one for the midrib (or spine), and one for front cross-section (Figure 4). These components are drawn in three orthogonal planes, being the boundaries in one that has the surface viewed from the top, the midrib in a plane viewed from the side, and the cross-section in a plane viewed from the front. The user delineates two template organs, which will be used as references to the creation of all plant organ variations that will be placed in the final arrangement (Figure 4).

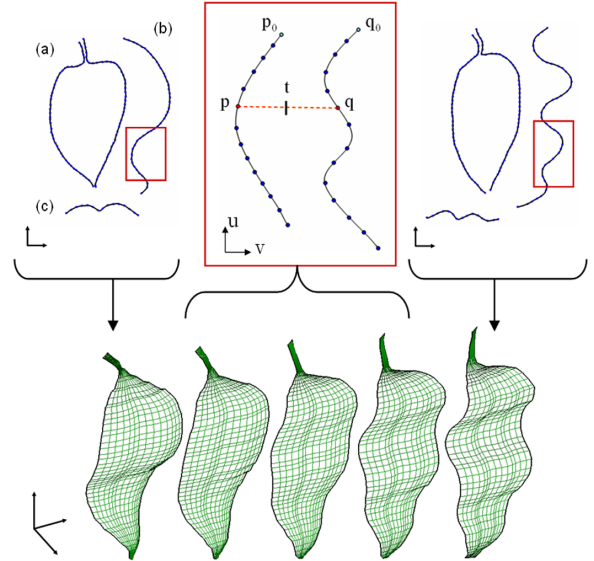


Figure 4: (Top row) Two plant organs, each defined by four 2D strokes sketched by the user: (a) left and right boundaries of organ (top view) and cross-sections for (b) side (organ midrib) and (c) front views. (Bottom row) Two organ surfaces created from the original sketched strokes and three in-betweens created from their linear interpolation. The red box on top row shows an example of sections of the midrib stroke being interpolated.

#### 4.1 Stroke capturing

After being re-sampled, the strokes are converted to a B-spline curve using the technique proposed by Cherlin *et al.* [2005]. This technique consists in using, for the conversion, the *Reduce-Resolution* algorithm [Samavati and Bartels 2004]. This algorithm applies reverse Chaikin subdivision to the given points, reducing their number by around a half and converting them into the control points of a quadratic B-spline. The resulting control points corresponds to a coarse representation of the original curve positioned in such a way that turns out to be a very close description of the initial shape. The detail part of the subdivision is constituted basically by noise produced by the innate imprecision from the input device

and is simply discarded. The algorithm is applied three consecutive times over the re-sampled points of the stroke before rendering the final B-spline representation. The number of iterative applications of the filtering algorithm was determined empirically, aiming at having fewer control points and keeping the curve close to the intended shape sketched by the user.

From the obtained quadratic B-spline representation, some equally separated points along their  $u$ -coordinates are calculated. These points, called *anchor points*, define the curve resolution and are used in the construction of the organ's 3D mesh. They can be seen as the dots in the top row of Figure 4. Their number can be arbitrarily specified when they are sampled and, for this application, the initial value is the number of control points obtained from filtering.

The strokes of both reference organs must have the same resolution. In our method, the spine stroke (Figure 4(b)) which has the largest number of anchor points gives both organs'  $u$  resolution. The  $v$  resolution is given by the cross-section stroke (Figure 4(c)) which, correspondingly, has the largest number of anchor points.

## 4.2 Surface modeling

In our system, the tessellation of the surface mesh is performed right after all strokes are sketched and it consists in using two techniques proposed by Cherlin *et al.* [2005]. The strokes for the boundaries and the cross-section are used to create a *cross sectional blending* surface. The *orthogonal deformation* operation is also applied using the spine stroke. An example of the resulting surfaces can be seen in Figure 4.

In a real plant, an organ hardly is completely identical to another. The same observation holds for most artistic botanic drawings. Therefore, we propose a simple mechanism to create variation in the modeled organs. The variation is controlled by the user when the organ is sketched. As mentioned before, two samples are drawn. Each of them defines one extreme of a linear interpolation. In this manner, the organs placed in the final arrangement will have an intermediate shape between the two user-defined templates. The interpolation of the organs is done in sketch space. Hence, what is interpolated is not the 3D surface, but the generative 2D sketch strokes. In consequence, the result is simply a new set of strokes, which determines the surface to be tessellated. The interpolation is processed for each *anchor point* (Section 4.1) in the pair of strokes. This is given by  $p_i = (1-t)p + tq, 0 < t < 1$ , where  $p_i$  is the resulting anchor point (Figure 4, top row) and  $p, q$  are the current anchor points from the first and second sketched strokes, respectively. Figure 4 (bottom row) shows a sequence of three interpolated organs with  $t = 0.25, 0.5$ , and  $0.75$ .

## 5 Phyllotactical arrangement

Our goal now is to place the lateral organ surfaces in a phyllotactical arrangement around the stem. *Phyllotaxis* is the classification of how organs (i.e. leaves, petals, needles) in a plant are arranged around a stem. It is commonly divided into *alternate*, *spiral*, *opposite* (*decussate*) and *whorled* patterns [Yotsumoto 1993]. Based on Figure 1, the focus of this system is modeling arrangements that follow the *spiral* pattern, which occurs very often in nature [Prusinkiewicz and Lindenmayer 1990].

A phyllotactical model defines an angle between every two consecutive organs along the stem. This angular distance is called *divergence angle* and is represented by  $\theta$  (Figure 5(a, b)). In the spiral case, the value of the divergence angle is the *Fibonacci angle*, also

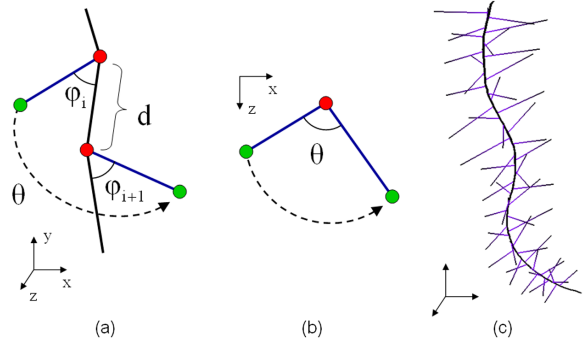


Figure 5: (a) Scheme of positioning measures for lateral organ placement: spiral phyllotactical pattern (indicated by dashed arrow and  $\theta$ ), internode distance  $d$ , and branching angle  $\varphi$ . (b) Top view of divergence angle  $\theta$  (c) The 3D organ reference lines arranged in the spiral phyllotactical pattern along the entire stem.

called *golden angle*, which is  $137.5^\circ$ . Therefore, in our system, every organ is placed  $137.5^\circ$  apart from the previous one, around the main axis in counter-clockwise direction, from the top to the bottom. As shown in Figure 5(a), every organ is also displaced along the stem in relation to its predecessor (Section 6). Although we select as default the spiral phyllotactical arrangement, other alternate patterns can also be used by simply changing the value of the divergence angle, as, for example, *monostichous* ( $30^\circ$ ), *distichous* ( $180^\circ$ ), *tristichous* ( $120^\circ$ ), and *tetrastichous* ( $90^\circ$ ) [Yotsumoto 1993]) (Figure 6).

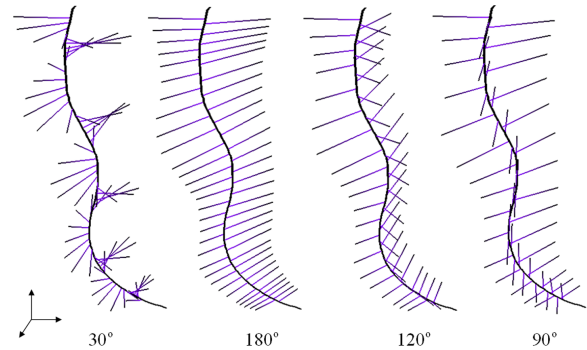


Figure 6: Examples of alternate phyllotactic patterns and their correspondent divergence angle  $\theta$  applied to the 3D extent of organs along the same stem shown in Figure 5.

## 6 Organ positioning

At this stage, our system creates a 3D representation directly from the 2D plant structure sketched by the user (Section 3), to allow 3D organ surfaces (Section 4) to be arranged in phyllotactical patterns (Section 5). Three main steps are performed: (1) find the node position (organ origin  $B_0$ ) along the stem; (2) find three key intersection points from the 2D plant structure:  $P_L$ ,  $P_R$  (branching intersections with the left and right boundary lines, respectively), and  $P_C$  (intersection of line  $P_L P_R$  and the stem line); and (3) find the organ tip location ( $B_1$ ) around the stem for a given phyllotactical divergence angle  $\theta$ . The resulting line  $B_0 B_1$  defines the 3D organ reference line (Figure 5(c)), that is later used in the mapping of the 3D organ surface (Section 7). Each of these three steps is described next.

## 6.1 Node position

The origin of each organ along the stem is called *node* and is given by  $B_0(x_0, y_0, 0)$  (Figure 7). The *internode distance*  $d$  (Figure 5(a)) is used to incrementally calculate  $B_0$  along the stem line where each organ must be placed. In our system, the internode distance is calculated independently for each layer in two steps: (1) computing the chord length of the stem between the points where it intersects the current inclination lines (points  $P_i$  and  $P_{i+1}$  in Figure 7); (2) dividing this length by the number of organs in a layer, which is selected by the user.

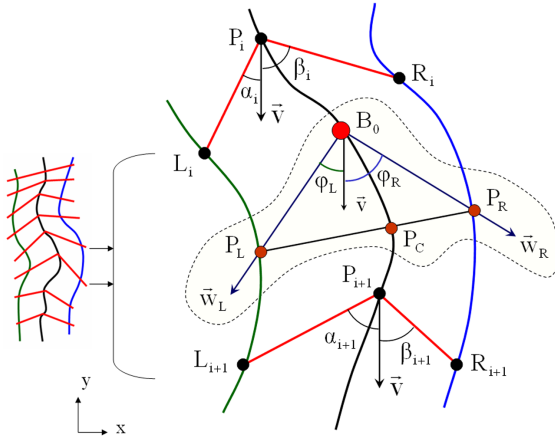


Figure 7: Scheme of drawing measurements for a given organ inside of a layer (as shown by the left side).  $B_0$  is position where the organ is being placed,  $L_iP_iR_i$  and  $L_{i+1}P_{i+1}R_{i+1}$  are the upper and bottom segments, respectively, that define a layer from the user sketch. From them, all the other necessary measures are calculated.

## 6.2 Branching intersections

At this stage, our system finds three branching intersection points  $P_L(x_l, y_l, 0)$ ,  $P_R(x_r, y_r, 0)$  and  $P_C(x_c, y_c, 0)$  (Figure 7) that are used to find the organ tip  $B_1(x, y, z)$  later on (Figure 8). The intersection calculations are between 2D vectors and the 2D line segments of the re-sampled original sketched lines (Section 3). For each inclination line  $i$ , we find its intersection points  $P_i$  with the stem line, and  $L_i$ ,  $R_i$  with the left/right boundary lines, respectively.

We then compute  $\alpha_i$  and  $\beta_i$ , the branching angles to the left and right sides of the stem at  $P_i$ , respectively.  $\alpha_i$  and  $\beta_i$  are computed as the  $\arccos$  of the dot product between  $\vec{v} = (0, -1, 0)$  and the vectors  $P_iL_i$  and  $P_iR_i$ , respectively. We then compute the branching angles to the left and right sides of the stem as  $\varphi_L = \alpha_i + (1-s)(\alpha_{i+1} - \alpha_i)$  and  $\varphi_R = \beta_i + (1-s)(\beta_{i+1} - \beta_i)$ , respectively, where  $s$  is the arc length from the beginning of the stem at  $P_i$  down to the organ position  $B_0$  divided by the arc length of the stem section from  $P_i$  until  $P_{i+1}$ .

Finally, our method finds  $P_L$  and  $P_R$ , the branching intersection points of vectors  $\vec{w}_L$  and  $\vec{w}_R$  with the left and right boundary lines, respectively. The vectors  $\vec{w}_L$  and  $\vec{w}_R$  are given after rotating  $\vec{v}$  by  $\varphi_L$  and  $\varphi_R$  degrees, respectively. The last point to be computed,  $P_c$  is the intersection point of line  $P_LP_R$  and the stem section from  $P_i$  until  $P_{i+1}$ .

## 6.3 Organ tip

Our system then computes  $B_1$ , which represents the tip of the organ connected to  $B_0$  at the stem (Figure 8).  $B_1$  is located in the 3D perimeter revolving the stem line at  $P_C$  by  $\theta'$  degrees, which is equal to  $\theta'$  of the previous node above the current  $B_0$  plus the divergence angle  $\theta$  (Section 5).

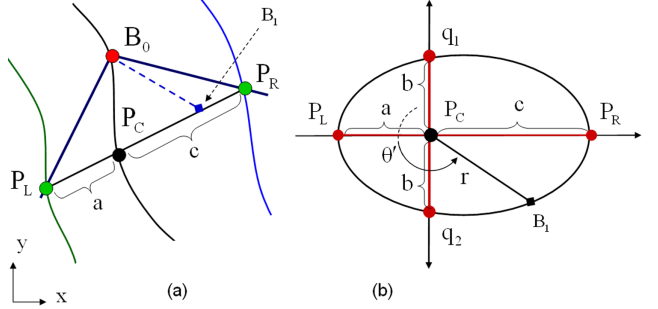


Figure 8: Computing  $B_1$ , the tip of the organ connected to  $B_0$  at the stem. (a) Original 2D sketch and measurements in the  $xy$ -plane; (b) Top view of revolving shape around  $P_C$  in a plane perpendicular to  $xy$ -plane and passing through  $P_L, P_C, P_R$ .

Notice that  $P_L, P_C$  and  $P_R$  are in the  $xy$ -plane of the input strokes and to have symmetric interpretation of the third ambiguous dimension, the revolve plan must be perpendicular to the  $xy$ -plane and passing through  $P_L, P_C$  and  $P_R$ . We make a local coordinate frame in this plane by setting  $P_C$  as the origin and  $P_R - P_C$  as the direction of the first axis. The second axis as usual can be defined by rotating  $P_R - P_C$  around  $P_C$  by  $90^\circ$  in the same plane. This frame has been demonstrated in Figure 8(b). As an important property, we would like to determine  $B_1$  such that we obtain a smooth revolve from  $P_L$  to  $P_R$  and vice-versa. This property is inspired by the roundness of plant structures. To dictate this property, we used a simple technique based on fitting two half-ellipses as demonstrated in Figure 8. To calculate these half-ellipses, we use the described local frame (Figure 8(b)). We begin by computing the distances  $a = \|P_L - P_C\|$ ,  $c = \|P_C - P_R\|$  (Figure 8) and then the average distance  $b = (a+c)/2$ , resulting in points  $q_1(0, -b)$  and  $q_2(0, b)$  (Figure 8(b)). Both half-ellipses are centered at  $P_C$ . If  $90^\circ \leq \theta' < 270^\circ$  then we consider the first half-ellipse passing through the points  $q_1, P_L, q_2$  with radius  $r^2 = (b^2 a^2)/(b^2 \cos^2 \theta' + a^2 \sin^2 \theta')$ . Now if  $0^\circ \leq \theta' < 90^\circ$  or  $270^\circ \leq \theta' < 360^\circ$ , then we consider the second half-ellipse passing through the points  $q_2, P_R, q_1$  with radius  $r^2 = (b^2 c^2)/(b^2 \cos^2 \theta' + c^2 \sin^2 \theta')$ . Therefore, the coordinates of  $B_1$  are computed as  $r \cdot \cos(\theta')$  and  $r \cdot \sin(\theta')$ , respectively. Finally, using the standard frame transformation, we find the coordinates of  $B_1$  in the original frame Figure 8(a).

## 7 Organ surface mapping and rendering

Finally, the organ can be properly placed in the stem using frame transformation. For the created 3D organ (Section 4), a local (normalized) coordinate frame is determined. As shown in Figure 9, this is given by  $(e_1, e_2, e_3, P_0)$ , where  $e_1 = (1, 0, 0)$ ,  $e_3$  is the organ reference line  $P_0P_1$ ,  $e_2 = e_3 \times e_1$ , and  $P_0$  is the organ origin. The desired position, direction, and orientation of this organ in the arrangement are given by another (normalized) coordinate frame  $(e'_1, e'_2, e'_3, B_0)$ , where  $e'_2$  is the vector from the next node position  $b$  and the current one  $B_0$ ,  $e'_3$  is the vector from the organ's current position  $B_0$  to its perimeter position  $B_1$  in the oval revolving the

stem line,  $e'_1 = e'_2 \times e'_3$ , and  $B_0$  is the current node position for the organ being placed. Once the bases are defined, the organ's surface is rotated and translated to the plant structure, and then scaled to fit its reference line  $B_0B_1$  by the scale factor  $s = \|B_0B_1\|/\|P_0P_1\|$ .

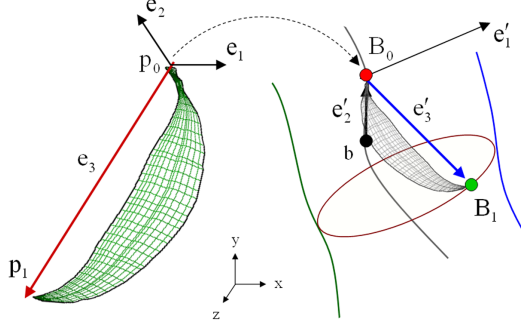


Figure 9: Local coordinate frames for an organ (left) and the position in the arrangement where it will be mapped (right). The basis vectors are shown before being normalized.

In our system, all rendering calls use OpenGL. The surface boundaries and silhouettes of each organ are rendered as line drawings to approximate traditional pen-and-ink renditions of concept drawings. We used the *edge buffer* data structure [Buchanan and Sousa 2000] for boundaries and silhouette extraction. Visibility processing uses the Z-buffer, with the polygons rendered in the background color (white) and the lines in black. Z-buffer artefacts (due to inappropriate clipping or hidden lines) are avoided by following the approach of Rössl *et al.* [2000] and Sousa and Prusinkiewicz [2003]. It consists in slightly translating the strokes along the vertex normal. This significantly reduces the stroke artefacts without compromising the quality of the results. In some cases, such artefacts create a desirable effect such as gaps at the boundaries and silhouettes, which are found in traditional concept drawings.

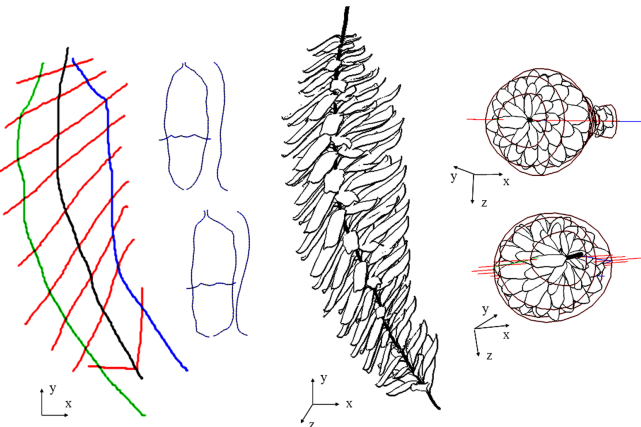


Figure 10: Approximation of a real botanical illustration of a white pine cone of Figure 1. (Left to right) 2D sketches for the pine cone structure and pair of pine needle structural elements. Side and top views of resulting 3D model with 20 needles per layer. Refer to Figure 17(a) (color plate).

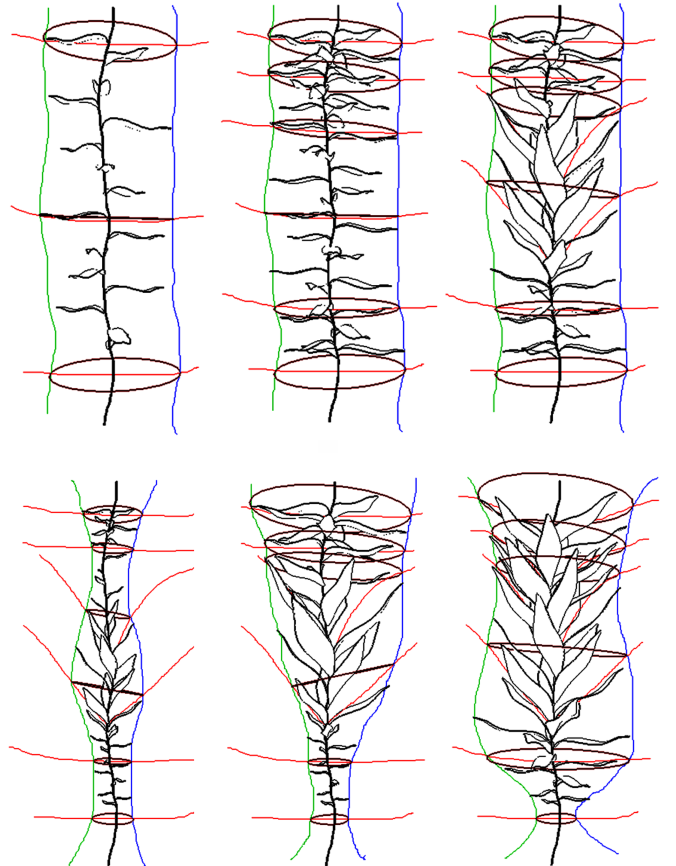


Figure 11: Various effects as a result of editing (in 2D) the inclination and boundary lines (top and bottom rows, respectively).

## 8 Results and discussions

All the results were generated on a 2.8GHz Pentium 4 with 1GB of RAM and a GeForce FX 5200 128MB video card, and using a mouse and a tablet as input devices.

Figures 10 and 17(a) (color plate) show a result after sketching the lateral construction lines of the real botanical illustration of Figure 1 (a). Pine needles were sketched by observing the shape of the hand-drawn needles also from Figure 1. Twenty nodes were distributed per layer along the stem. Note in Figure 10 the three different 3D views of the final result. For the top view, the original construction lines are now displayed in 3D. This feature was inspired by observing Figure 1(b) where internal organs are drawn in conjunction with previously sketched construction lines. Our system allows for the exact same thing but in 3D. Inclination lines are processed and displayed to approximate the roundness of plant structures, exactly in the same way as described in Section 6. We observed that this feature turned out to be a valuable resource for visualizing, editing and correcting the resulting 3D plant arrangement. The user selects a particular construction line by clicking on it and the original 2D sketch is displayed for editing. After editing in 2D the entire 3D arrangement is re-adjusted and displayed.

Effects of editing inclination and boundary construction lines are shown in Figure 11. Figures 12 and 17(c) (color plate) illustrate the five phyllotactic patterns implemented in our system. Figure 13 shows the effect of increasing the number of organs along the stem and alternating the pattern from spiral to *monostichous*.

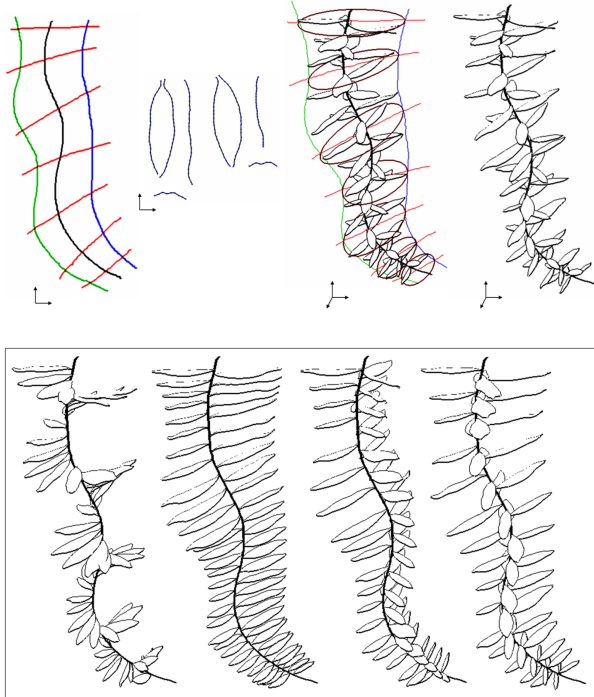


Figure 12: Phyllotactic patterns. (Top row) The 2D plant structure and a pair of organ (leaf) structures. The resulting 3D model with leaves arranged in a spiral phyllotactical pattern with construction lines on and off. (Bottom row) Other alternate phyllotactical patterns (left to right) *monostichous* ( $30^\circ$ ), *distichous* ( $180^\circ$ ), *tristichous* ( $120^\circ$ ), and *tetrastichous* ( $90^\circ$ ). Refer to Figure 17(c) (color plate).

Figures 14 and 17(b) (color plate) illustrate an approximation to the modeling and traditional rendering of a *Bromeliaceae*. Figure 15 shows a similar approximation of foliage. In both figures, all construction lines for the plant structures and lateral organs were sketched by looking at a real botanical illustration of the plants. In both figures, the complete sets of construction lines are displayed. Also, their final composition was performed interactively by simply translating the rendered image of each of the two plant parts. In the future we plan to provide 3D assembling capabilities for multiple modeled plants for constructing more complex plant arrangements and ecosystems.

Figure 16 illustrates different phyllotactic patterns and construction lines displayed over the 3D model. Figure 17 (color plate) repeats Figure 10 and 14 and presents another result for the five phyllotactic patterns.

The results show that our approach produces models corresponding closely to what the user expects (i.e., “what you sketch is what you get”) with images similar to traditional ink line drawings found in traditional botanical illustrations.

## 9 Conclusions and future work

This paper contributes towards making plant modeling an easier task and proposes a new approach to sketch-based modeling. The technique is relatively simple and tries to follow and adapt the already well established knowledge of artists in the subject. It allows

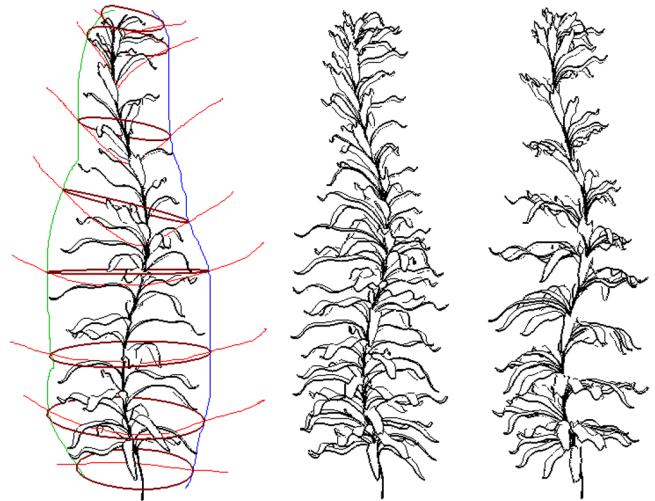


Figure 13: (Left) Spiral phyllotactical arrangement of plant with construction lines displayed. (Middle) Removing construction lines and increasing the number of lateral organs. (Right) Switching to a *monostichous* ( $30^\circ$ ) phyllotactical pattern.

fast development of specific 3D plant models and can be a more natural interface than the ones available nowadays.

We are currently investigating several important issues. The current system is fairly specialized, dedicated to a single type of plant arrangement. Nonetheless, it uses a new technique that can be properly expanded to other plant structures and domains. We also observed that undesired intersections between organs in the final 3D plant arrangement might happen and should be detected and corrected. Different factors that influence the plant organs positioning and variation should also be considered. Finally, a more in-depth understanding of specific botanical illustration processes and general artistic variation and the generalization to other more complete plant types are also important additions to be investigated in the future.

## Acknowledgments

We would like to thank the anonymous reviewers for the important and constructive comments and suggestions received. We also thank Eleanor B. Wunderlich for providing her botanical illustrations used in our experiments, and Patricia Rebolo Medici for her useful artistic advice. This work was supported in part by Discovery Grants from the Natural Sciences and Engineering Research Council of Canada and by an iCORE Graduate Student Scholarship.

## References

- BOUDON, F., PRUSINKIEWICZ, P., FEDERL, P., GODIN, C., AND KARWOWSKI, R. 2003. Interactive design of bonsai tree models. *Computer Graphics Forum (Proc. of Eurographics '03)* 22, 3, 591 – 599.
- BUCHANAN, J., AND SOUSA, M. C. 2000. The edge buffer: a data structure for easy silhouette rendering. In *Proc. of NPAR '00*, 39–42.

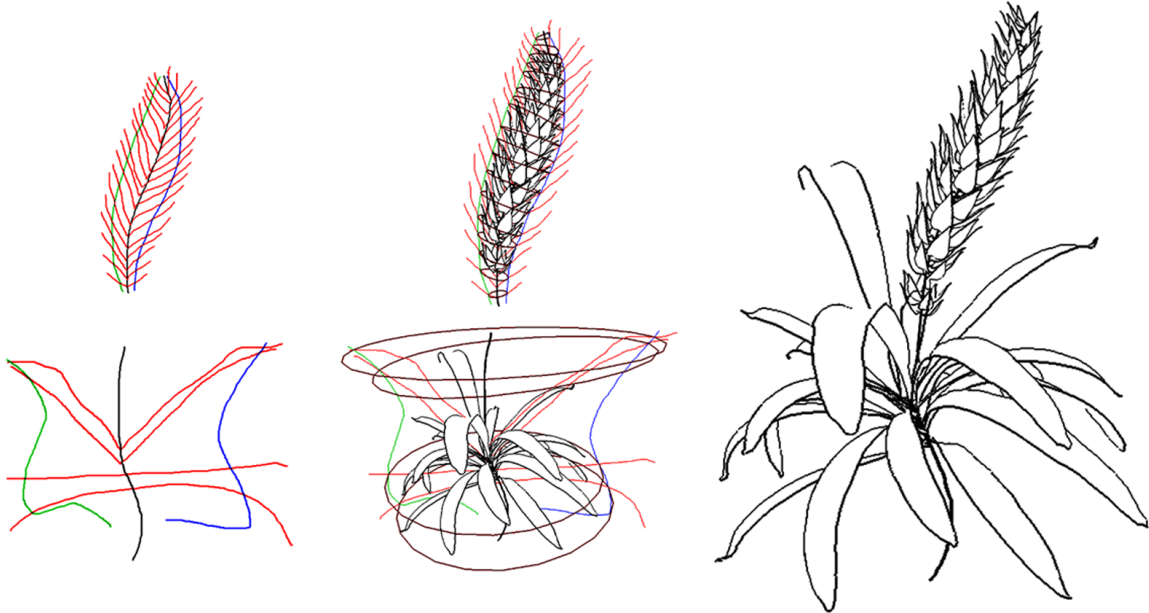


Figure 14: Approximating the modeling and traditional pen-and-ink line rendering of a *Bromeliaceae*. Refer to Figure 17(b) (color plate).

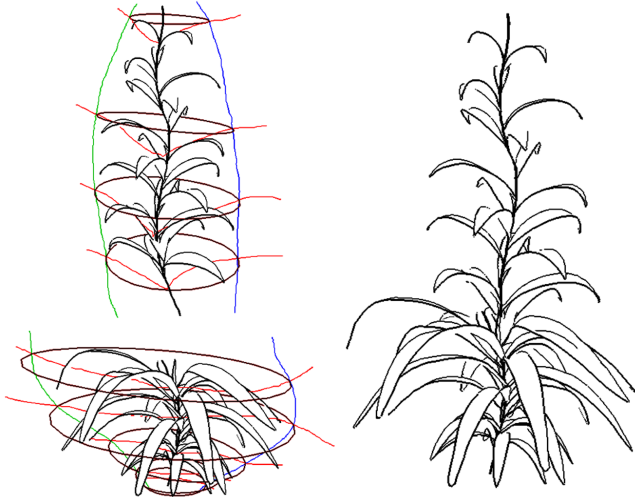


Figure 15: Approximating the modeling and traditional pen-and-ink line rendering of foliage.

CHERLIN, J. J., SAMAVATI, F., SOUSA, M. C., AND JORGE, J. A. 2005. Sketch-based modeling with few strokes. In *Proc. of the 21st Spring Conference on Computer Graphics (SCCG '05)*, 132–140.

DEUSSEN, O., AND STROTHOTTE, T. 2000. Computer-generated pen-and-ink illustration of trees. In *Proc. of SIGGRAPH '00*, 13–18.

DI FIORE, F., VAN HAEVRE, W., AND VAN REETH, F. 2003. Rendering artistic and believable trees for cartoon animation. In *Proc. of Computer Graphics International (CGI '03)*, 144–151.

HODGES, E., Ed. 2003. *The Guild Handbook of Scientific Illustration*. John Wiley and Sons. ISBN: 0471360112.

IGARASHI, T., AND HUGHES, J. F. 2001. A suggestive interface for 3D drawing. In *14th annual ACM symposium on User interface software and technology (UIST'01)*, 173–181.

IGARASHI, T., MATSUOKA, S., AND TANAKA, H. 1999. Teddy: A sketching interface for 3d freeform design. In *Proc. of SIGGRAPH 99*, 409–416.

IJIRI, T., OWADA, S., OKABE, M., AND IGARASHI, T. 2005. Floral diagrams and inflorescences: interactive flower modeling using botanical structural constraints. *ACM Transactions on Graphics (Proc. of SIGGRAPH '05)* 24, 3, 720–726.

JIRASEK, C., PRUSINKIEWICZ, P., AND MOULIA, B. 2000. Integrating biomechanics into developmental plant models expressed using l-systems. In *Plant Biomechanics 00*, 615–624.

LINTERMANN, B., AND DEUSSEN, O. 1999. Interactive modeling of plants. *IEEE Computer Graphics and Applications* 19, 1, 56–65.

MECH, R., AND PRUSINKIEWICZ, P. 1996. Visual models of plants interacting with their environment. In *Proc. of SIGGRAPH '96*, 397–410.

NAYA, F., JORGE, J. A., CONESA, J., CONTERO, M., AND GOMIS, J. M. 2002. Direct modeling: from sketches to 3D models. In *Proc. of the First Ibero-American Symposium in Computer Graphics (SIACG '02)*, 109–117.

NEALEN, A., SORKINE, O., ALEXA, M., AND COHEN-OR, D. 2005. A sketch-based interface for detail-preserving mesh editing. *ACM Transactions on Graphics (Proc. of SIGGRAPH '05)* 24, 3, 1142–1147.

OKABE, M., AND IGARASHI, T. 2003. 3D modeling of trees from freehand sketches. In *GRAPH '03: Proc. of the SIGGRAPH 2003 conference on Sketches & applications*, 1–1.

OKABE, M., OWADA, S., AND IGARASHI, T. 2005. Interactive design of botanical trees using freehand sketches and example-

based editing. *Computer Graphics Forum (Proc. of Eurographics '05)* 24, 3, 487–496.

PEREIRA, J. P., BRANCO, V. A., JORGE, J. A., SILVA, N. F., CARDOSO, T. D., AND FERREIRA, F. N. 2004. Cascading recognizers for ambiguous calligraphic interaction. In *Proc. of First Eurographics Workshop on Sketch-Based Interfaces and Modeling (SBIM '04)*, 63–72.

PRUSINKIEWICZ, P., AND LINDENMAYER, A. 1990. *The Algorithmic Beauty of Plants*. Springer-Verlag, New York. ISBN: 0387972978.

PRUSINKIEWICZ, P., MUENDERMAN, L., KARWOWSKI, R., AND LANE, B. 2001. The use of positional information in the modeling of plants. In *Proc. of SIGGRAPH '01*, 289–300.

RAWSON, P. 1987. *Drawing*. University of Pennsylvania Press. ISBN: 0812212517.

RÖSSL, C., KOBBELT, L., AND SEIDEL, H. 2000. Line art rendering of triangulated surfaces using discrete lines of curvature. In *Proc. of WSCG '00*, 168–175.

SALISBURY, M. P., WONG, M. T., HUGHES, J. F., AND SALESIN, D. H. 1997. Orientable textures for image-based pen-and-ink illustration. In *Proc. of SIGGRAPH '97*, 401–406.

SAMAVATI, F. F., AND BARTELS, R. H. 2004. Local filters of b-spline wavelets. In *Proc. of International Workshop on Biometric Technologies (BT '04)*, University of Calgary, 105–111.

SECORD, A. 2002. Weighted voronoi stippling. In *Proc. of NPAR '02*, 37–43.

SOUSA, M. C., AND PRUSINKIEWICZ, P. 2003. A few good lines: Suggestive drawing of 3D models. *Computer Graphics Forum (Proc. of Eurographics '03)* 22, 3, 327 – 340.

SOUSA, M. C. 2005. Computer tools for the science illustrator - what do you need? In *The Guild of Natural Science Illustrators (GNSI), 2005 Annual Conference*. (Invited Presentation and Panel Discussion).

STROTHOTTE, T., PREIM, B., RAAB, A., SCHUMANN, J., AND FORSEY, D. R. 1994. How to render frames and influence people. *Computer Graphics Forum (Proc. of Eurographics '94)* 13, 3, 455–466.

WEBER, J., AND PENN, J. 1995. Creation and rendering of realistic trees. In *Proc. of SIGGRAPH '95*, 119–128.

WUNDERLICH, E. 1991. *Botanical Illustration in Watercolor*. WatsonGuptill, New York. ISBN: 0823005305.

YANG, C., SHARON, D., AND VAN DE PANNE, M. 2005. Sketch-based modeling of parameterized objects. In *Proc. of 2nd Eurographics Workshop on Sketch-Based Interfaces and Modeling (SBIM '05)*, 63–72.

YOTSUMOTO, A. 1993. A diffusion model for phyllotaxis. *Journal of Theoretical Biology* 162, 131–151.

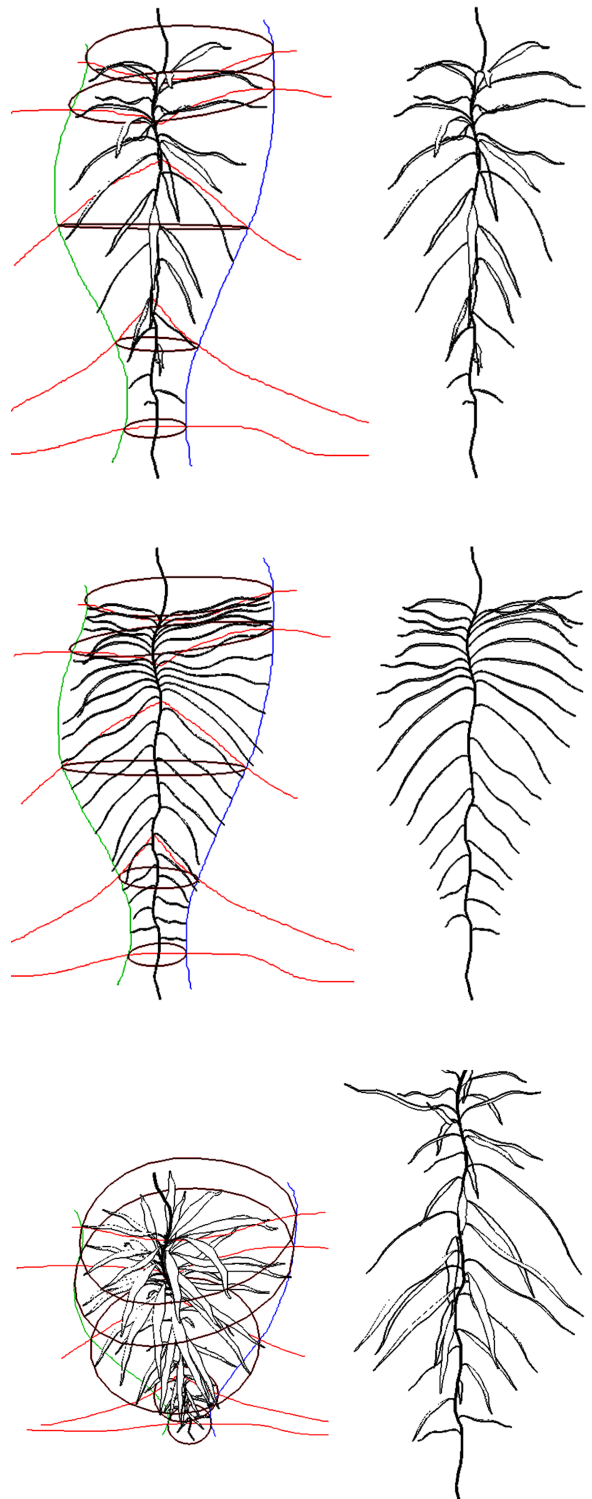
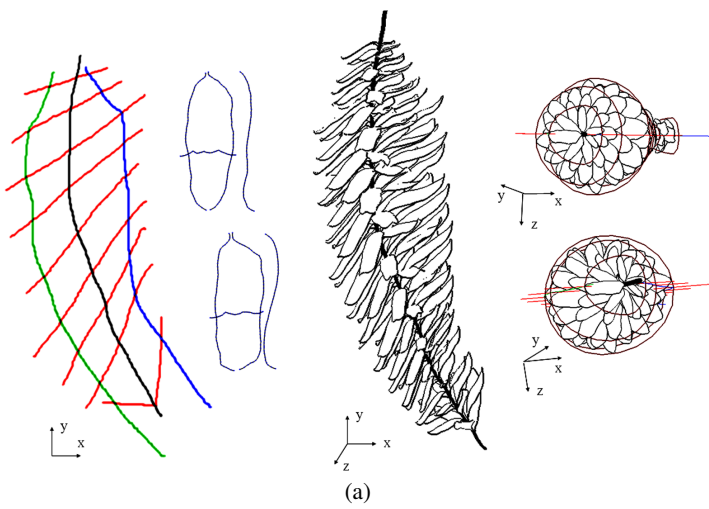
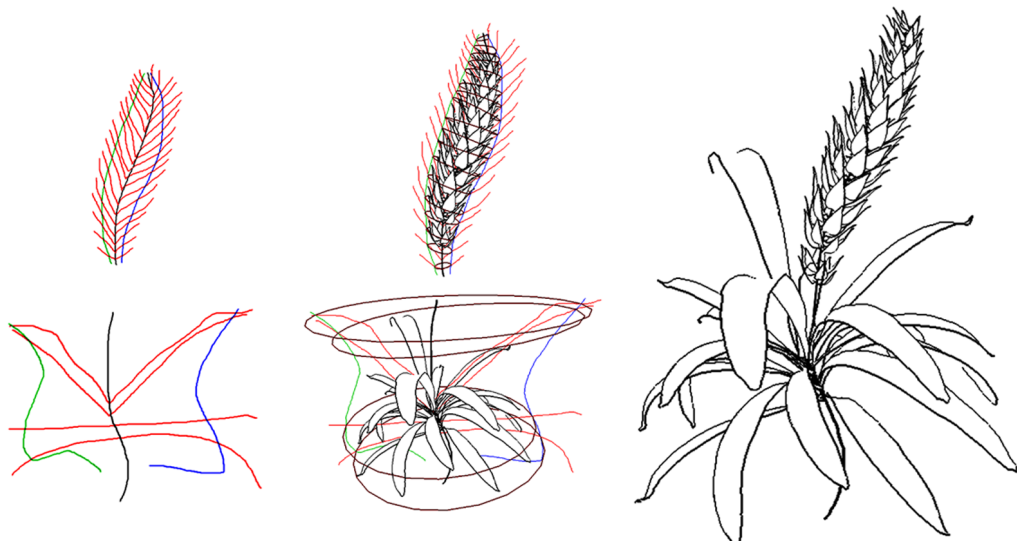


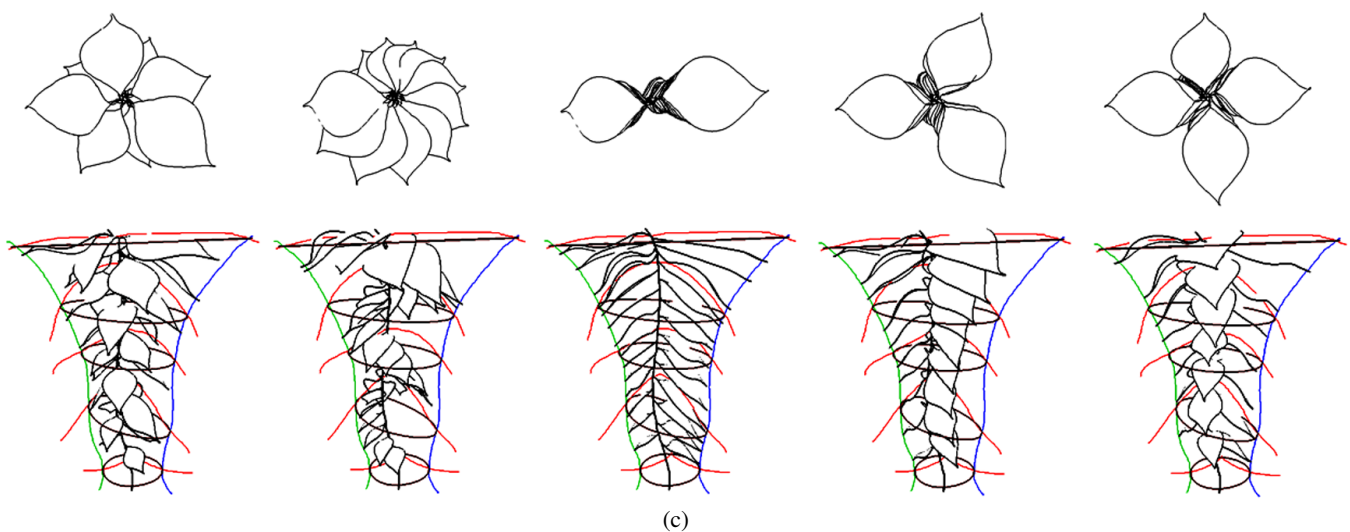
Figure 16: Different visualizations of phyllotactic patterns. Refer to Figure 17(c) (color plate).



(a)



(b)



(c)

Figure 17: (a) 2D sketches for the pine cone and needles. Side and top views of resulting 3D model. (b) Approximating the modeling and traditional pen-and-ink line rendering of a *Bromeliaceae*. (c) Different visualizations of phyllotactic patterns (left to right): spiral, monostichous, distichous, tristichous, and tetrastichous.